JOURNAL OF NEUROTRAUMA XX:1–12 (XXXX XX, 2020)

DOI: 10.1089/neu.2019.6949

Original Article

Improved Functional Recovery in Rat Spinal Cord Injury Induced by a Drug Combination Administered with an Implantable Polymeric Delivery System

Andrea Bighinati,[1] Maria Letizia Focarete,[2,3] Chiara Gualandi,[3] Micaela Pannella,[5] Alessandro Giuliani,[1] Sarah Beggiato,[4] Luca Ferraro,[4,5] Luca Lorenzini,[1] Luciana Giardino,[1,2,5] and Laura Calzà[2,5,6]

Abstract

Spinal cord injury (SCI) is an incurable condition, in which a cascade of cellular and molecular events triggered by inflammation and excitotoxicity impairs endogenous regeneration, namely remyelination and axonal outgrowth. We designed a treatment solution based on an implantable biomaterial (electrospun poly (L-lactic acid) [PLLA]) loaded with ibuprofen and triiodothyronine (T3) to counteract inflammation, thus improving endogenous regeneration. *In vivo* efficacy was tested by implanting the drug-loaded PLLA in the rat model of T8 contusion SCI. We observed the expected recovery of locomotion beginning on day 7. In PLLA-implanted rats (i.e., controls), the recovery stabilized at 21 days post-lesion (DPL), after which no further improvement was observed. On the contrary, in PLLA + ibuprofen (Ibu) + T3 (PLLA-Ibu-T3) rats a further recovery and a significant treatment effect were observed, also confirmed by the gait analysis on 49 DPL. Glutamate release at 24 h and 8 DPL was reduced in PLLA-Ibu-T3– compared to PLLA-implanted rats, such as the estimated lesion volume at 60 DPL. The myelin- and 200-neurofilament–positive area fraction was higher in PLLA-Ibu-T3–implanted rats, where the percentage of astrocytes was significantly reduced. The implant of a PLLA electrospun scaffold loaded with Ibu and T3 significantly improves the endogenous regeneration, leading to an improvement of functional locomotion outcome in the SCI.

Keywords: glutamate; ibuprofen; myelination; secondary neurodegeneration; thyroid hormone

Introduction

Spinal cord injury (SCI) causes disability and death and represents a severe medical, social, and economic burden at global level.[1] Incidence varies from 15 to 45 cases per million, a figure which translates to 2.5 million people are living with SCI, with >130,000 new injuries reported annually. In spite of the impressive advancements in the medical and surgical treatments of these critical patients, and although a large body of pre-clinical evidence has been accumulated on cellular and molecular mechanisms occurring during the very early phase of the lesion, SCI is still considered an incurable condition. Routine protocols for the acute phase are presently aimed at reducing edema. Although some drugs, approved for other neurological diseases, are currently being tested (e.g., riluzole, Nogo-A targeting drugs, Rho inhibitor, cethrin, and minocycline), none currently appear to be effective in rescuing the sensory and motor functions.

The pathophysiology of SCI includes different phases following a defined time frame.[2] The primary phase develops within minutes and continues for 8–12 h.[3] The ischemic damage, reflecting the trauma suffered (contusion, compression, and shear injury), is characterized by elevation of excitatory amino-acid extracellular levels and tissue inflammation, including infiltration of neutrophils and macrophages; these cells promote a series of self-propagating events determining the secondary phase (or secondary injury), which is a predictor of long-term SCI morbidity and mortality. It is sustained by the inflammatory cell cascade, involves astrocytes and microglial cells, and is characterized by demyelination progression, scar formation, neurodegeneration, and central cavitation.[4] This well-established phenomenon in experimental SCI is now recognized and described in humans by magnetic resonance imaging, including its self-propagation.[5,6]

Given that the inflammatory response characterizing the acute phase is a recognized primary therapeutic target in SCI, the use of

[1]Department of Veterinary Medical Sciences, [2]Health Sciences and Technologies (HST) CIRI-SDV, [3]Department of Chemistry "Giacomo Ciamician" and National Consortium of Materials Science and Technology (INSTM, Bologna RU), [6]Pharmacy and Biotechnology, Alma Mater Studiorum–University of Bologna, Bologna, Italy.
[4]Department of Life Sciences and Biotechnology, Section of Medicinal and Health Products, University of Ferrara, Ferrara, Italy.
[5]Iret Foundation, Ozzano Emilia, Emilia, Italy.

anti-inflammatory drugs has been extensively proposed. However, steroid administration is still disputed because of the small benefit/risk ratio of these drugs. Actually, this approach is being abandoned and considered a ''harmful standard of care'' in many trauma centers.[7,8] The systemic administration of various nonsteroidal anti-inflammatory drugs (NSAIDs) is not associated with a significant improvement in locomotor function, and, similarly, no effective therapies for reducing secondary neurodegeneration are available.[4,9] We envisaged that a main reason underlying the current failure in SCI pharmacological treatment could be the monotherapy approach, which seems inadequate to break the vicious cycle between excitotoxicity, increased inflammation, impaired remyelination, and neurodegeneration. Along these lines, we hypothesized that an approach based on the combination of an anti-inflammatory drug plus a remyelinating agent could act on two key points of the complex SCI pathological cascade. Thus, we selected ibuprofen (Ibu), whose systemic administration has been widely tested for acute SCI in pre-clinical studies, as an anti-inflammatory drug.

In fact, besides to inhibit cyclooxygenase activity, Ibu decreases the activation of RhoA, a key enzyme impeding axonal sprouting after axonal damage.[10] This dual activity is potentially unique in the context of the double-edged-sword role of inflammation in SCI and has formed the rational basis for a clinical study aimed at repurposing Ibu in the treatment of SCI.[11] As a promyelinating agent, we selected the active form of thyroid hormone (TH), triiodothyronine (T3). T3 is a key component of the molecular machinery permitting the maturation of non-myelinating oligodendrocyte precursor cells (OPCs) into myelinating oligodendrocytes (OLs), maturation which is blocked during inflammation.[12–14] After that, our laboratory proposed TH systemic administration to improve remyelination in inflammatory-demyelinating diseases; different and independent rodent and non-human-primate studies have confirmed that exogenous TH administration is effective in overcoming the OPC differentiation blockade, in protecting myelin and axons, finally ameliorating the clinical outcome in a different experimental model.[15–17]

A pharmacological strategy based on the combination of Ibu and T3 to target two main pathogenic events in acute SCI (i.e., inflammation and demyelination) faces, however, major obstacles in the necessity of drug systemic administration. For instance, it seems probable that high Ibu doses are necessary to inhibit central nervous system (CNS) RhoA activity, thus rendering this approach likely burdened with severe side effects.[18] Similarly, prolonged systemic administration of T3 exposes the patient to the risk of hyperthyroidism. To overcome these issues, we designed a polymeric delivery system based on a polylactic acid–based biodegradable scaffold (poly [L-lactic acid]; PLLA) loaded with the two drugs, to be implanted at the lesion site immediately after the lesion occurrence and ensuring a controlled and prolonged drug release rate.

In this study, we demonstrated that an Ibu- and T3-loaded electrospun scaffold, when implanted *in vivo* in the contusion SCI rat model, reduces glutamate release, tissue inflammation, and astroglial reaction at 24 h and 8 days post-lesion (DPL); over the long term, it reduces lesion volume and improves the morphological indices of myelination and axonal injury (55 DPL), finally improving long-term locomotor outcome.

Methods

See also the Supplementary Materials and Methods.

Animals and study design

CD/Sprague-Dawley female rats ($N = 86$; 200–250 g; Charles River, Calco, Italy) were used. All animal protocols described here were carried out according to European Community Council Directives 2010/63/UE, approved by the Italian Ministry of Health (D.Lgs 26/2014, authorization no. 574/2015-PR). Moreover, animal protocols were carried out in compliance with the ARRIVE (Animal Research: Reporting of In Vivo Experiments) guidelines and the NIH Guide for the Care and Use of Laboratory Animals. Animals underwent a contusive spinal cord lesion at the thoracic level, T9. Rats were pre-medicated with enrofloxacin and tramadol (5 mg/kg, subcutaneously [s.c.]) and then anesthetized with isoflurane (1–3%) in O_2. The contusive lesion of the spinal cord was obtained using an Impact One impactor (Leica Microsystems GmbH, Wetzlar, Germany), using a 1.5-mm-diameter cylindrical tip with a force of 1 N and 0 sec of stance time; the depth of impact was 1.5 mm. After performing the spinal cord lesion, PLLA scaffolds, either conjugated or unconjugated with drugs, were locally implanted and coated with surgical adhesive (BioGlue; CryoLife, Kennesaw, GA).

This proof-of-concept study was aimed at reducing secondary injury in SCI, by the controlled, local delivery of two drugs achieved by implanting a drugs-loaded biomaterial at the spinal cord lesion site (Fig. 1A). The expected therapeutic effect on locomotion recovery of the drugs-loaded PLLA, also considering efficacy parameters of other pre-clinical studies aimed to limit secondary degeneration, was established as $\geq$20% compared to drugs-unloaded PLLA. On this basis, and also considering the most used locomotion readout in published data, the power analysis for the sample-size calculation was performed by considering the improvement of the Basso, Beattie, and Bresnahan (BBB) scale as the primary end point.[19] For $\alpha = 0.05$, power (1-b) = 0.80, and an effect size (d) = 1.12, 14 animals per group were required (G* Power 3.1.9.2 software). A randomized surgery list was generated, to assign the rats to the two cohorts (i.e., PLLA and PLLA-Ibu-T3), and a further randomization in each cohort was performed at the euthanization, assigning the animals to the different exploratory endpoint experiments (flow cytometry, molecular biology, histology, and immunohistochemistry; Fig. 1B,D). We also pre-determined inclusion/exclusion criteria for lesion efficacy. According to the BBB scale guidelines, in order to obtain a moderate-severity lesion in all animals, rats with a BBB score $\geq$15 at day 3 after lesion were excluded. On this basis, 1 rat from the PLLA group was excluded from the study.

To test the hypothesis supporting the new drug formulation, we euthanized animals at three time points. To verify whether the PLLA-Ibu-T3 scaffold counteracts glutamate excitotoxicity and inflammation, we euthanized two groups of animals at 24 h and 8 DPL, respectively, to analyze glutamate release from synaptosomal preparations and inflammatory cellular infiltrate at the lesion site. To verify whether the PLLA-Ibu-T3 scaffold applied in the acute post-trauma phase ameliorates anatomical and functional outcome, we performed the last locomotion tests (BBB score and gait analysis), histological measurement of the lesion volume, plus immunohistochemistry (IHC) analysis of microglia and astrocyte reaction, myelin, and axon damage at long-term post-lesion.

Scaffolds preparation

Scaffolds of PLLA were produced by co-electrospinning two different solutions and collecting the corresponding fibers evenly distributed on a rotating collector. The delivery system containing T3 and Ibu was produced by co-electrospinning two different PLLA solutions, one containing a suitable amount of Ibu to give a 5-wt percentage of drug in the final fibers and the other one containing a suitable amount of T3 to give a 0.6-wt percentage of drug in the final fibers. An electrospun control sample was produced by

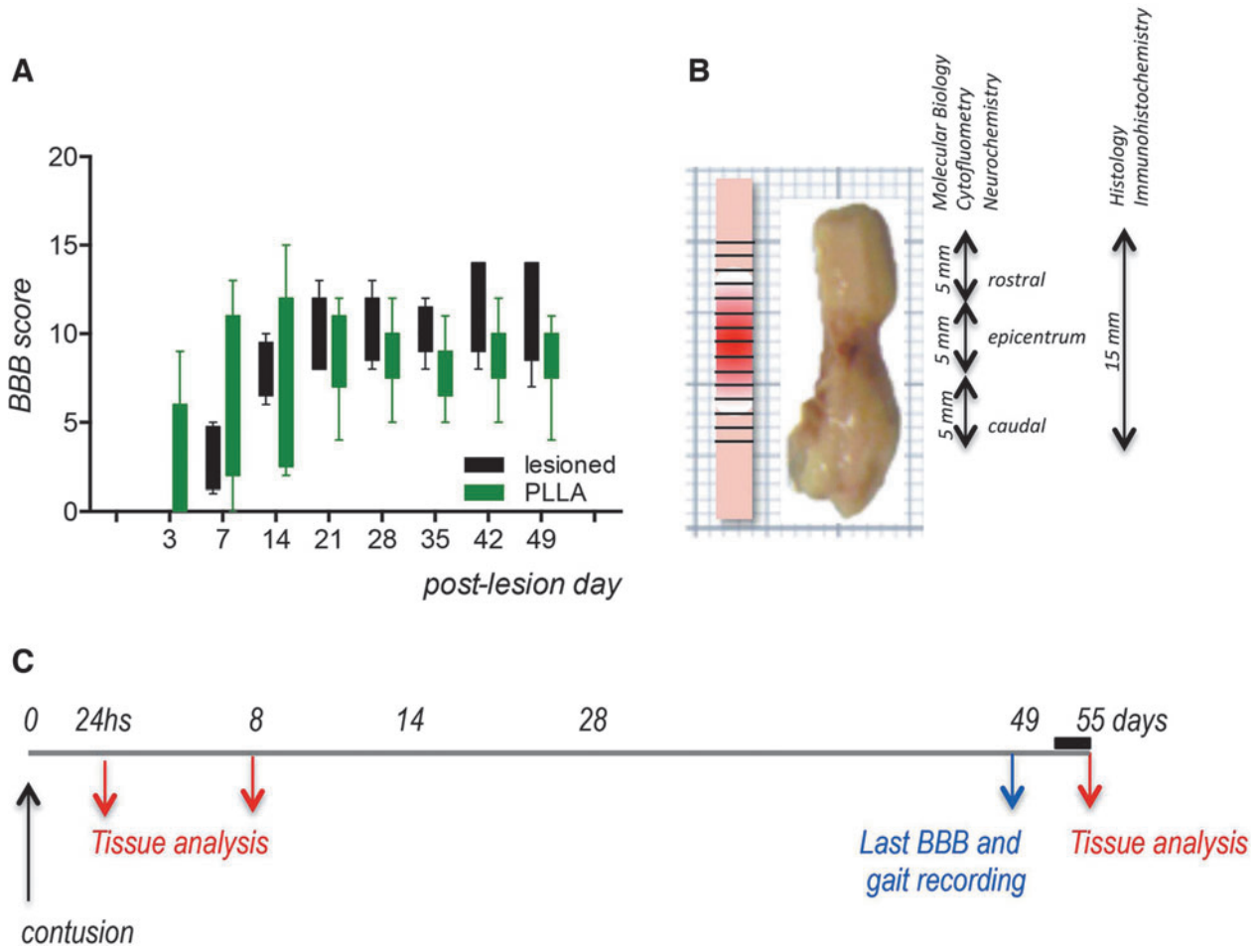

FIG. 1. Study design and pilot experiment. (**A**) Results from the pilot study to establish the most appropriate control group, showing the BBB score in lesioned (black) and lesioned rats implanted with PLLA, alone (green). (**B**) Sampling schema for tissue processing. (**C**) Experimental schedule pointing on the timing for tissue and biological fluids analysis (red arrows) and last locomotion testing (blue arrow). BBB, Basso, Beattie, Bresnahan Locomotor Rating Scale; Ibu, ibuprofen; PLLA, poly (L-lactic acid); T3, triiodothyronine.

co-electrospinning the aforementioned described polymeric solutions not loaded with drugs. Scaffolds were sterilized using gamma rays (25 KGy) before implantation.

Drug analytical procedure

Drug release from the PLLA was measured *in vitro* as described in the Supplementary Materials. Briefly, rectangular electrospun samples were immersed in phosphate-buffered saline (PBS; 0.1 M, pH = 7.4) and incubated in a shaking water bath at 37°C for a maximum period of 15 days. At regular intervals, PBS was completely removed and replaced with fresh buffer. Aliquots were analyzed by means of high-perfermance liquid chromatography/ultraviolet and mass spectrometry to determine Ibu and T3 release, respectively. The results are reported as cumulative release.

Locomotion analysis

To evaluate loss of hindlimb function, 15 animals per group were used at the time point of 60 DPL. The BBB score was evaluated before spinal cord lesion, 3 DPL, and then once per week until animal euthanization. One animal retained normal locomotion after spinal cord lesion and failed to show gait deficit and was excluded from the study.

Gait analysis was performed using the CatWalk (Noldus, Wageningen, The Netherlands) automatized system. Animals were trained to walk repeatedly along the platform before surgery, then tested 2 days before spinal cord lesion and at 14, 28, and 49 DPL. Gait analysis was evaluated using the following parameters: print area, maximum contact area (spatial parameters), stride length, step cycle (comparative parameters), stand time, swing time, swing speed, single stance (kinetic parameters), duty cycle, step sequence regularity index, and cadence (coordination parameters).

Histology and immunohistochemistry

Tissue analysis was carried out in paraffin or cryostat sections, using EE and toluidine blue staining, and IHC.

Flow cytometry

A 10-mm spinal cord segment enclosing the injury site was processed for flow cytometry. Briefly, animals were euthanized and perfused with 100 mL of Dulbecco's modified PBS (DPBS; Lonza, Basel, Switzerland) in order to remove circulating inflammatory cells. Cells were isolated with the Adult Brain Dissociation Kit solutions and GentleMACS Octo Dissociator (Miltenyi Biotec, Bergisch Gladbach, Germany). At least 2×10^5 cells were suspended in DPBS. Cell populations were marked respectively with CD11b-PE-Vio770 (1:10), CD45-APC-Vio770 (1:10), GLAST-PE (1:10), CD32-APC (1:10), and CD86-VioBright-FITC (1:10) for the identification of macrophagic ($CD11^+CD45^+$), microglial

($CD11^+CD45^-$), lymphocitic ($CD11^-CD45^+$), astrocytic ($GLAST^+$), and M2 lineages ($CD32^-/CD86^-$; Miltenyi Biotec). In order to distinguish live cells, 4′,6-diamidino-2-phenylindole staining solution (0.1 μg/mL) was used. Immunolabeled cell-count analysis was made by MACSQuant Analyzers and FlowLogic software (Miltenyi Biotec).

Synaptosome preparation, glutamate, and gamma aminobutyric acid assay

See the Supplementary Material.

RNA isolation, reverse transcription real-time polymerase chain reaction, and real-time polymerase chain reaction

Total RNA isolation was performed by using the RNeasy Micro kit (Qiagen, Milan, Italy), following the manufacturer's instructions. First-strand complementary DNAs (cDNAs) were obtained using the iScript™cDNA Synthesis Kit (Bio-Rad Laboratories, Hercules, CA). An RNA sample with no reverse-transcriptase enzyme in the reaction mix was processed as a no-reverse transcription control sample. Semiquantitative real-time polymerase chain reaction (PCR) was performed using the CFX96 real-time PCR system (Bio-Rad).

Statistical analysis

Results were expressed as mean ± standard error (SEM) and plotted on graphs. Statistical analyses were performed using Prism software (GraphPad v7; GraphPad Software Inc., La Jolla, CA). Student's *t*-test was used for comparison of two groups and ordinary one-way analysis of variance (ANOVA) and post-hoc test for comparison of more than two groups. BBB score and gait analysis data have been analyzed using the two-way ANOVA test. Results were considered significant when the probability of their occurrence as a result of chance alone was <5% ($p < 0.05$).

Data and materials availability

All raw data, materials, images, videos, and analysis generated for this study are available on request.

Results

Poly (L-lactic acid) electrospun nanofibers guaranteed the expected ibuprofen and triiodothyronine release profile over time

To realize the dual-drug delivery system in a translational perspective, we used two marketed drugs together with biodegradable polymers already approved by the U.S. Food and Drug Administration (FDA) for derma filling and endovasal scaffolds that have been manufactured as electrospun fibers. Polymeric electrospun scaffolds were designed and manufactured in order to guarantee a release rate of Ibu and T3, starting within the first 24 h after injury and continuing for at least 8–10 DPL, to prevent/limit secondary neurodegeneration. To prepare a dual-drug delivery electrospun system, Ibu and T3 were individually encapsulated by ''direct blending'' in different polymeric solutions, which were simultaneously coelectrospun on the same collector to give a fibrous scaffold consisting of differently loaded fibers. Drug release was measured as indicated in the Methods (see also Supplementary Materials). This scaffold released 48 μg/mL of Ibu over 14 days, with an estimated daily release of 3.4 μg/mL, and 50 ng/mL of T3, with an estimated daily release of 3.5 ng/mL.

The poly (L-lactic acid)/ibuprofen/triiodothyronine scaffold counteracted molecular and cellular events elicited in the acute spinal cord injury (24 h and 8 days post-lesion)

The contusion model of SCI in rats was used to test efficacy. According to the ARRIVE guidelines, a pilot study ($N = 9$ animals per group) was performed to determine the most appropriate control group, by comparing lesioned animals to lesioned animals implanted with PLLA without drugs, expecting PLLA to be an inactive component of the proposed therapeutic solution. The BBB score, established as the primary end point of the efficacy study, was subsequently used for this pilot study also. Given that no differences were observed in the BBB score during the observational time (two-way ANOVA, treatment effect, $F_{(1,\ 127)} = 1.171$; $p = 0.2813$; 49 DPL; Fig. 1A), the control, sham-operated group consisted of rats lesioned and implanted with drug-unloaded PLLA.

For the analysis of the main molecular and cellular mechanisms responsible for secondary degeneration onset, PLLA- and PLLA-Ibu-T3–implanted animals were euthanized at 24 h or 8 DPL (Fig. 1C). Figure 1B shows tissue collection details. First, glutamate release was measured from lesioned spinal cord synaptosomes ($N = 5$ animals per group). In the PLLA group, similar basal glutamate release was observed in synaptosomes from tissues dissected 24 h or 8 days after SCI (6.63 ± 1.35 and 6.87 ± 2.23 pmol/5 min/mg of protein, respectively; Fig. 2A). Basal glutamate release in synaptosomes from tissue dissected from the PLLA-Ibu-T3 group 24 h after SCI was significantly lower (3.72 ± 0.66 pmol/5 min/mg of protein) than that measured in the respective control group (PLLA group, 24 h; Fig. 2A). A tendency toward a similar effect was also observed in the PLLA-Ibu-T3 synaptosomes from tissue dissected 8 days after the lesion. In the PLLA group, K^+-evoked glutamate release was similar in rat spinal cord synaptosomes from tissue dissected 24 h and 8 days after the lesion (202 ± 23% and 205 ± 21% of basal values, respectively). K^+-evoked glutamate release in synaptosomes from tissue dissected from the PLLA-Ibu-T3 group 8 days after SCI was significantly lower (153 ± 4% of basal values) than that measured in the respective control group (PLLA group, 8 days; Fig. 2A).

Contrarily, K^+-evoked glutamate release in PLLA-Ibu-T3 synaptosomes from tissue dissected 24 h after the lesion (179 ± 13% of basal values) was comparable to that observed in the respective PLLA group (Fig. 2A). To verify whether the effect of PLLA-Ibu-T3 is specific for glutamate, we also analyzed synaptosomal gamma aminobutyric acid (GABA) release. In the PLLA group, similar basal GABA release was observed in synaptosomes from tissues dissected 24 h or 8 days after SCI (1.91 ± 0.60 and 2.31 ± 0.61 pmol/5 min/mg of protein, respectively; Fig. 2B). Comparable values were observed in synaptosomes from tissues dissected from the PLLA-Ibu-T3 group 24 h and 8 days after SCI (2.07 ± 0.4 and 3.04 ± 0.9 pmol/5 min/mg of protein, respectively; Fig. 2B). In the PLLA group, K^+-evoked GABA release was comparable in rat spinal cord synaptosomes from tissue dissected 24 h and 8 days after the lesion (166 ± 8% and 203 ± 21% of basal values, respectively). K^+-evoked GABA release in synaptosomes from tissue dissected from the PLLA-Ibu-T3 group 24 h and 8 days after SCI (193 ± 6% and 172 ± 10% of basal values, respectively) was similar to that observed in the PLLA group (Fig. 2B).

To verify whether the PLLA-Ibu-T3 scaffold regulates inflammatory cellular responses in the spinal cord, we analyzed cells expressing inflammation-related membrane markers by flow cytometry analysis ($N = 4$ animals per group). Results are presented in

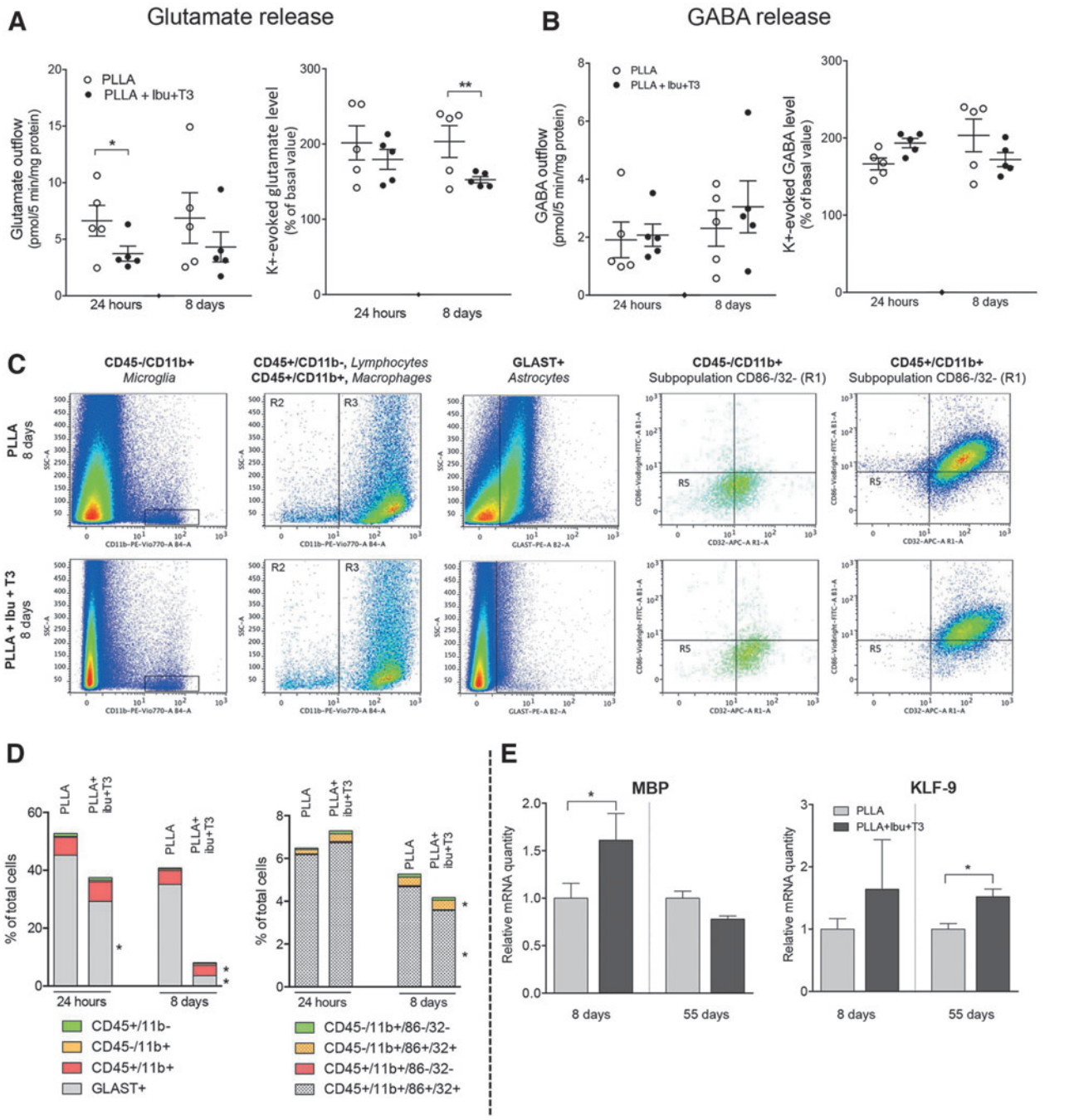

FIG. 2. PLLA-Ibu-T3 scaffolds reduce glutamate level and inflammatory cellular infiltrate at short term after lesion. (A,B) Spontaneous and K^+-evoked glutamate (**A**) and GABA (**B**) release from synaptosomal preparation in the spinal cord at 24 h and 8 days after contusion. (**C**) Representative plots of the analyzed cell population by flow cytometry from PLLA and PLLA-Ibu-T3 groups at 8 days. (**D**) Results from the flow cytometry analysis at 24 h and 8 days, expressed as percent value of total counted cells. (**E**) mRNA expression level of MBP and KLF-9 in the injured spinal cord, at 8 and 55 days after lesion. Statistical analysis: one-way ANOVA and post-hoc test, $*p \le 0.05$, $**p \le 0.01$ for three groups comparison; Student's *t*-test, $*p \le 0.05$, $***p \le 0.001$ for two groups comparison. ANOVA, analysis of variance; GABA, gamma aminobutyric acid; GLAST, glutamate aspartate transporter; Ibu, ibuprofen; KLF-9, Kruppel-like factor 9; MBP, myelin basic protein; mRNA, messenger RNA; PLLA, poly (L-lactic acid); T3, triiodothyronine.

Figure 2C,D, where a representative plot for each treatment (Fig. 2C) and means variations of the respective markers (Fig. 2D) are shown. At 8 DPL, the number and proportion of $CD45^+CD11b^+$, identified as macrophages and microglia-activated cells, were significantly reduced by the treatment (PLLA, $4.83 \pm 0.85\%$; PLLA-Ibu-T3, $3.60 \pm 0.47\%$; $p < 0.05$). Inactive microglia, marked with $CD45^{low}CD11b^+$, showed a non-significant reduction at 8 DPL in PLLA-Ibu-T3–implanted rats. Also, $CD45^+CD11b^-$ cells, which identify lymphocyte lineage, showed a non-significant trend toward reduction, and treatment-related differences were found in $CD45^-CD11b^+$ cells (microglial markers). We also investigated M1/M2 macrophage transition, using CD86 and CD32 as M1 markers

with respect to $CD45^+CD11b^+$ and $CD45^-CD11b^+$ cells. Flow cytometry data did not reveal any differences in CD86 and 32 positive cells in either group, but confirmed that the subpopulation of $CD45^+$ $CD11b^+$ cells is reduced in PLLA-Ibu-T3–implanted rats. Finally, we also analyzed glutamate/aspartate transporter (GLAST)-positive cells, which are considered as cells belonging to the astrocytic lineage, which significantly decreased in rats treated with PLLA-Ibu-T3 (PLLA = 36.43 ± 3.57%; PLLA-Ibu-T3, = 3.60 ± 1.26%; $p < 0.0001$).

As a fast readout to test the impact of reduced inflammation on remyelination, we investigated messenger RNAS (mRNA) expression level for myelin basic protein (MBP), the most abundant myelin protein, and for KLF-9 (Kruppel-like factor 9), a T3-responsive gene implicated in OPC terminal differentiation. Both markers were upregulated in PLLA-Ibu-T3– compared to PLLA-implanted rats (Fig. 2E).[20–22]

The poly (L-lactic acid)/ibuprofen/triiodothyronine scaffold improved functional recovery and mitigated spinal cord degeneration

Functional recovery in contused rats was monitored using the 21-point BBB scale (primary end point) and gait analysis. In the mild contusion model we used, bladder function was preserved.[23] BBB scale results are presented in Figure 3A as an interquartile range. According to the inclusion criteria of the study design, the PLLA groups included 14 rats, whereas the PLLA-Ibu-T3 group included 15 rats. Two-way ANOVA revealed a time-dependent recovery ($F_{(7,216)} = 16.57$; $p < 0.0001$), starting at day 7. In PLLA-implanted rats, the recovery stabilized at 21 DPL, after which no further improvement was observed. A significant treatment effect was observed ($F_{(7,216)} = 13.22$; $p = 0.0003$), at the analyzed time points (interaction, $F_{(7,216)} = 13.22$; $p = 0.003$). Notably, at the final observational time point (49 DPL), only 20% of PLLA-implanted rats achieved a BBB score $\geq$10, whereas 60% of PLLA-Ibu-T3 rats achieved a score of 10 and a further 27% achieved a score $\geq$15 (Fig. 3B). At 49 DPL, the BBB recovery rate was 54.2% in PLLA-Ibu-T3 compared to 37% in PLLA implanted rats.

Recovery of locomotion was also monitored by the gait analysis (automatic trace analysis), which allows the quantification of the spatial, kinetic, comparative, and coordinator parameters of both front and hind paws. Figure 3C shows representative traces and color-coded footprints from both groups, where warm colors correspond to higher pressure. The results of the quantitative gait analysis are shown in Figure 3D, where the main spatial, comparative, kinetic, and coordination parameters are illustrated. Statistical analysis was performed by the two-tailored non-parametric Mann-Whitney U test (95% confidence level). Many parameters were different in the two groups, with higher performance, such as print/contact area for both front and hind paws and stand time of hind paws, observed in the PLLA-Ibu-T3– compared to the PLLA-implanted rats. In particular, gait coordination strongly improved in PLLA-Ibu-T3–implanted compared to control rats, as indicated by the cadence and step regularity index.

We then analyzed the anatomical outcome of the treatment, by estimating lesion volume at euthanization ($N = 10$ rats per group). The spinal cord was coronally ($N = 5$ rats per group; Fig. 4B) and longitudinally ($N = 5$ rats per group; Fig. 4D) sectioned all over the rostrocaudal and dorsoventral extension of the lesion, respectively, and the area of lesion was measured at 15 levels and expressed as a percentage area. The lesion extension covered 10 mm in a rostrocaudal direction (Fig. 4A) and 2.5 mm in depth (Fig. 4C) in both groups. However, the estimated lesion volume in PLLA-Ibu-T3–implanted rats was significantly lower compared to PLLA rats (two-way ANOVA, treatment effect, rostrocaudal, $F_{(1,105)} = 6.854$, $p = 0.0101$; dorsoventral, $F_{(1,116)} = 8.553$, $p = 0.0041$). In particular, the treatment limited the severity of lesion extension caudal to the lesion *epicentrum* and also limited its ventral progression.

We then analyzed several parameters for long-lasting tissue inflammation, demyelination, astrocyte reaction, and neuroprotection, in the spinal cord rostrally (5.6–4.8 mm) and caudally (5.6–4.8 mm) to the lesion *epicentrum*, by IHC and image analysis ($N = 5$ rats/group animals). OX42-IR, which recognizes the CR3 complement receptor (CD11b/CD18) in microglia and macrophages, was used to analyze the persistent inflammatory tissue reaction in the white (dorsal *funiculus*) and gray (dorsal horn) matter (Fig. 5A–D). In both areas, both rostrally and caudally to the lesion, OX42-IR was lower in PLLA-Ibu-T3– compared to PLLA-implanted rats (Fig. 5E,F). The drug-loaded scaffold also reduced long-lasting astroglial reaction in the gray matter (ventral horn) in particular (Fig. 5G,H), as also shown in the high-mag micrographs illustrating the ventral horn (Fig. 5I,J) and image analysis performed in the white (dorsal *funiculus*) and gray matter (dorsal and ventral horn; Fig. 5K–M). Myelin distribution was analyzed using the lipophilic stain, FluoroMyelin™, that at low magnification illustrated the more uniform myelin distribution in PLLA-Ibu-T3 compared to PLLA (Fig. 5N,O, respectively), in particular in the lateral and ventral *funiculus*. The high-power micrographs (Fig. 5P,Q, respectively) illustrated the myelin sheath rarefaction, more evident in the inserts (p,q) obtained by applying a deconvolution procedure to the original image. The FluoroMyelin-positive area fraction measured in the dorsal, lateral, and ventral *funiculus* is presented in Fig. 5R–T. Finally, we investigated the potential axonal protection in the dorsal *funiculus* (see Fig. 5X for the sampled area), which is the spinal cord area more directly involved in the contusion lesion, by analyzing the NF200-IR (Fig. 5U,V). Residual F200-IR was much higher in PLLA-Ibu-T3– compared to PLLA-implanted rats (Fig. 5W).

Discussion

Functional outcome after a spinal cord trauma is determined by the physical characteristics of the impact and by the so-called secondary degeneration, which induces and supports the progressive and long-lasting degeneration of myelin and neurons, as well as tissue cavitation. The acute phase of the lesion is therefore a recognized target for limiting the functional deficit after SCI. The

FIG. 3. PLLA-Ibu-T3 scaffolds ameliorate the locomotor recovery. (**A**) BBB score in rat implanted with PLLA and PLLA-Ibu-T3. Statistical analysis: two-way ANOVA; the value indicates the treatment effect. (**B**) Percentage of rats showing a score higher than 10 and 15, respectively, at 49 days after the contusion injury. (**C**) Gait trace and footprints of representative rats from the two experimental groups. The code of the respective animal is indicated (#). (**D**) Spatial, comparative, kinetics, and coordination parameters of the gait analysis at 49 days after the injury. All data are expressed as mean + SEM, whereas cadence and step regularity index are reported as single rat value. Statistical analysis: Student's *t*-test, $*p < 0.05$; $**p < 0.001$. ANOVA, analysis of variance; BBB, Basso, Beattie, Bresnahan Locomotor Rating Scale; Ibu, ibuprofen; PLD, post-lesion days; PLLA, poly (L-lactic acid); SEM, standard error of the mean; T3, triiodothyronine.

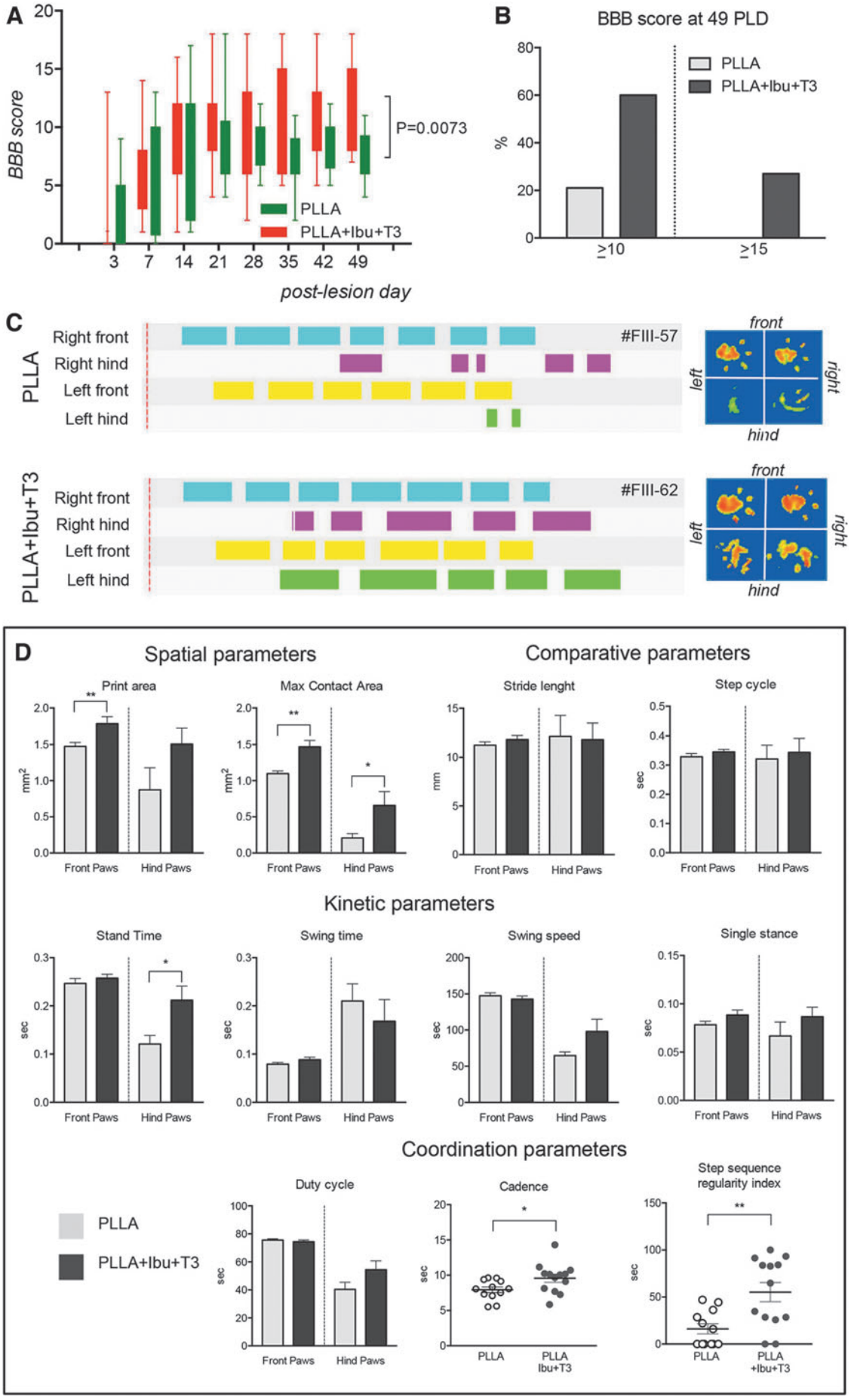

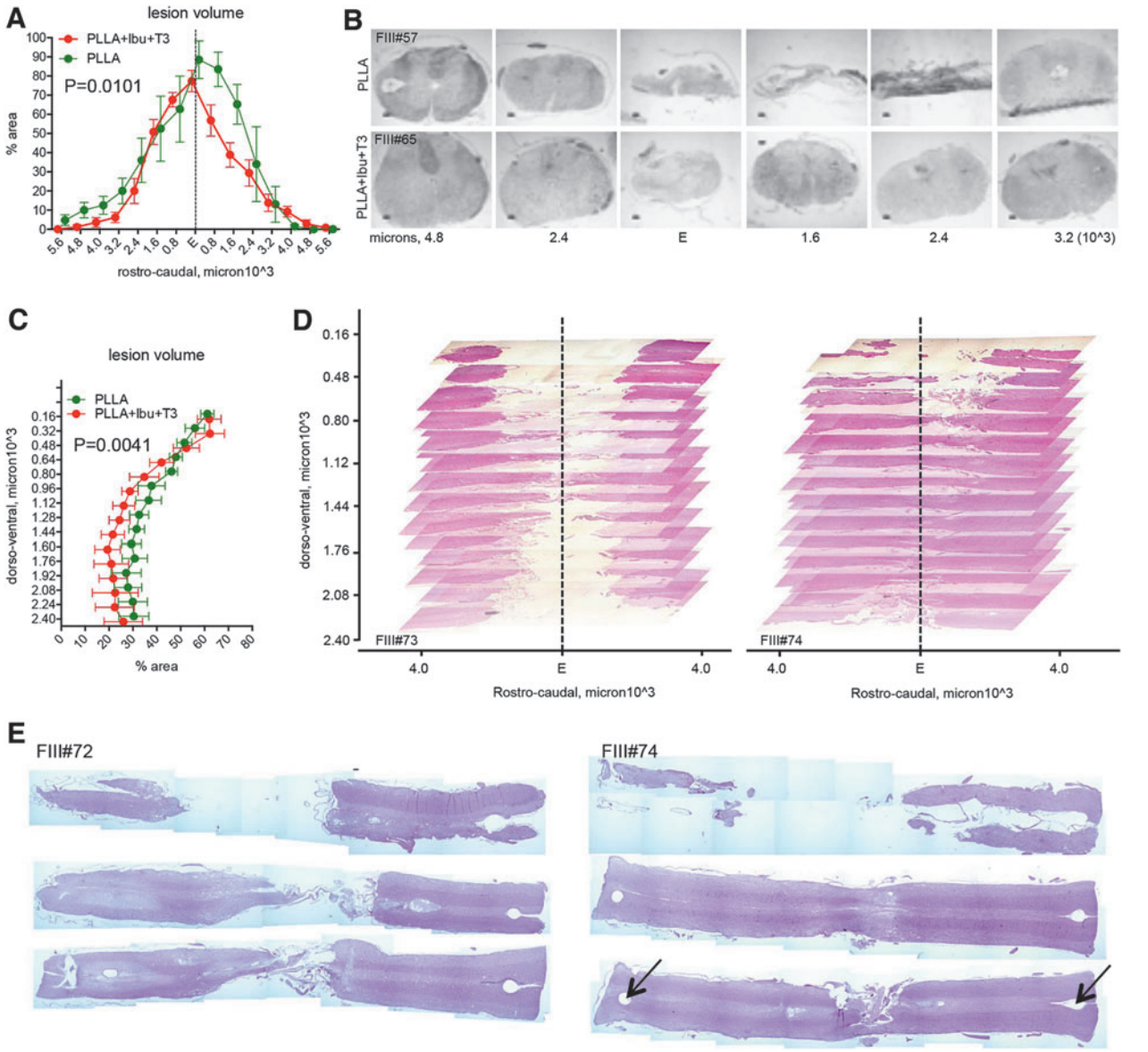

FIG. 4. PLLA-Ibu-T3 scaffolds reduces the spinal cord lesion extension. (**A**) Lesion extension calculated as lesioned area (%) in coronal section, over 11.2mm, rostrally and caudally to the lesion *epicentrum*. (**B**) Micrographs of toluidine blue stained coronal section at different rostrocaudal levels from representative rats in the two treatment groups. The animal code is indicated. (**C**) Lesion extension calculated as lesioned area (%) in longitudinal section (D), over the entire dorsoventral extension. (**D**) 3D reconstruction of the lesion by micrographs of EE-stained longitudinal section at different dorsoventral analyzed levels from representative rats in the two treatment groups. The animal code is indicated. (**E**) Power micrographs of EE representative stained longitudinal section at different dorsoventral levels from representative rats in the two treatment groups. The animal code is indicated. Statistical analysis: two-way ANOVA, the number refers to the treatment effect. 3D, three-dimensional; ANOVA, analysis of variance; Ibu, ibuprofen; PLLA, poly (L-lactic acid); T3, triiodothyronine.

complex molecular pathology and the limited CNS drug targeting make systemic monotherapy often inadequate for limiting secondary neurodegeneration. In this proof-of-concept study, we provide evidence that a drug combination composed by Ibu and T3 locally delivered by electrospun PLLA scaffold implanted in the spinal cord immediately after the lesion, and providing a long-lasting drug release, improves locomotion and gait coordination, resulting in a recovery rate of 46% higher compared to control, at the late observational time (49 DPL). Moreover, we demonstrated that the PLLA-Ibu-T3 scaffold improves remyelination, as indicated by the increased MBP mRNA expression level, and overcomes the OPC differentiation block, as indicated by the KLF-9 upregulation.

The two marketed drugs, Ibu as anti-inflammatory drug, T3 as promyelinating and neuroprotective agent, and an FDA-approved biomaterial for implant in humans (PLLA), were chosen given that the study was designed to exploit drugs repositioning, combinatory therapy, and the translational potential.

NSAIDs, and in particular Ibu, has attracted great interest for the treatment of neurological diseases, currently being tested in several clinical trials. In the context of human SCI, Ibu has been indicated as a plausible strategy for the pharmacological augmentation of

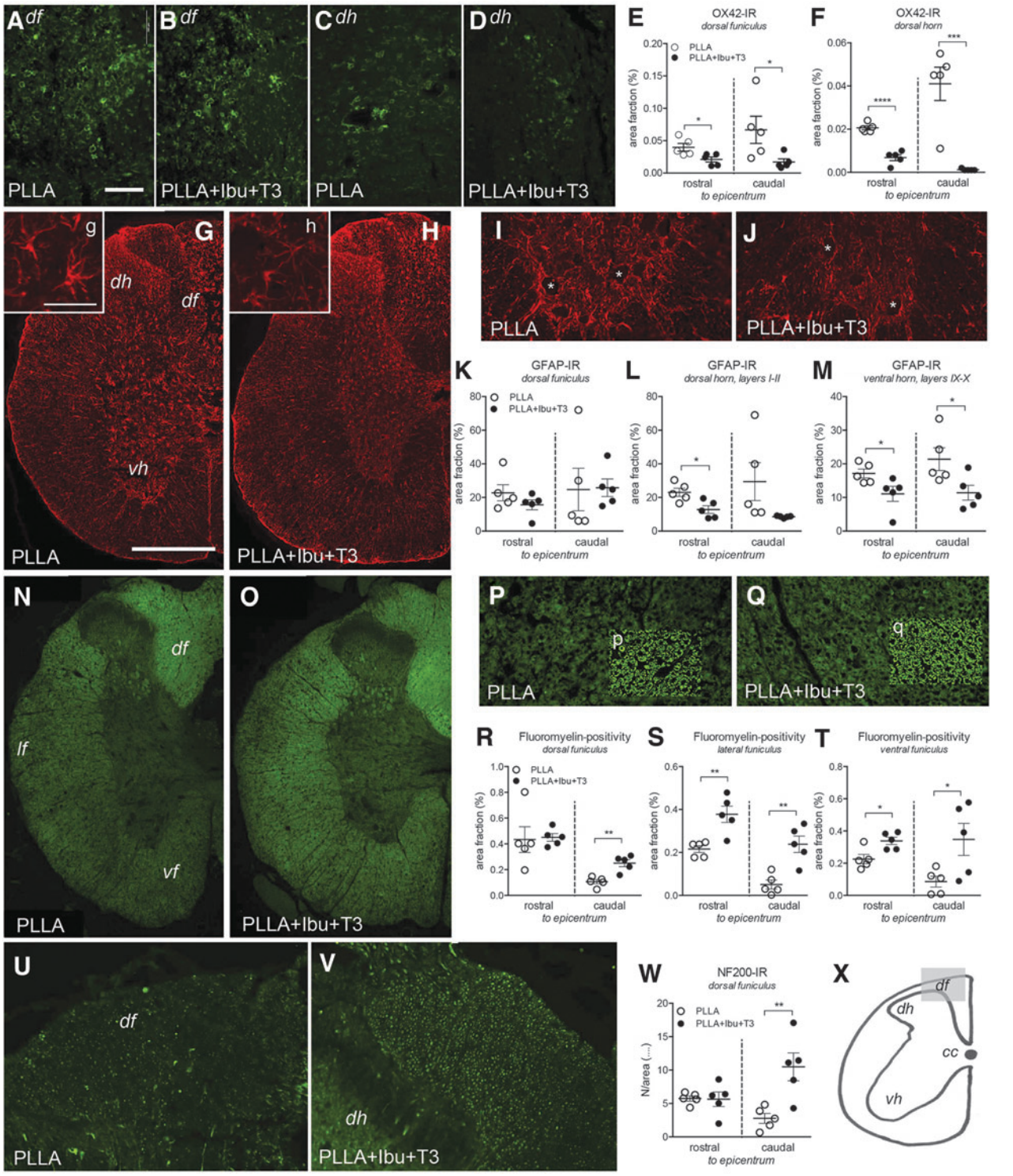

FIG. 5. PLLA-Ibu-T3 scaffolds reduces long-lasting inflammation, scar reaction, and axonal degeneration and increases myelin indices. (**A–D**) Representative micrographs of OX42-IR microglial cells in the white and gray matter. (**E,F**) Quantitative evaluation of the OX42-IR expressed as area fraction. (**G–J**) Representative micrographs of GFAP-IR astrocytes in spinal cord hemisections (G,H) also showing the astrocyte morphology (g,h) and in the ventral horn (I,J). (**K–M**) Quantitative evaluation of the GFAP-IR expressed as area fraction. (**N–Q**) Representative micrographs of FluoroMyelin staining in spinal cord hemisections (N,O) also showing the myelin sheat (P,Q) as highlighted by deconvulted inserts (p,q). (**R–T**) Quantitative evaluation of FluoroMyelin staining expressed as area fraction. (**U,V**) Representative micrographs of NF200-IR in the dorsal funiculus. (**W**) Quantitative evaluation of the NF200-IR expressed as number of dots in the sampled area. Schema illustrating the sampled area. Bars: (G,H,N,O) 1 mm; (A–D,I,J,P,Q,U,V 100 μm. Statistical analysis: Student's *t*-test, $*p < 0.05$; $**p < 0.01$; $***p < 0.001$. Ibu, ibuprofen; PLLA, poly (L-lactic acid); T3, triiodothyronine; df, dorsal funiculus; dh, dorsal horn; lf, lateral funiculus; vf, ventral funiculus; vh, ventral horn.

neurorehabilitation and has been included in the phase I SCISSOR clinical trial (NCT02096913).[11,24] Pre-clinical studies in which Ibu was systemically administered have provided contrasting results. In particular, in one study, long-term administration of Ibu (60 mg/kg/d, twice per day, over 42 days), reduced microglial reactivity early on, but failed to improve functional recovery, and no histological sign of neuroprotection was observed. [25] In another study, long-term s.c. Ibu delivery by an osmotic minipump (filled with 500 mg of Ibu, 2.5 μL/h for 28 days, releasing 70 mg/kg/d) led to a 28% improvement of the BBB scale.[26]

Other studies in which Ibu was orally administered showed no effect on histological or functional outcome, even in combinatory therapies.[27] These contrasting results have been, at least partially, explained by the limited Ibu CNS targeting; despite the fact that free Ibu rapidly crosses the blood–brain barrier, plasma protein binding limits the vascular-corrected brain concentration to 1–2% by reducing the free fraction in the bloodstream.[18,28] Moreover, severe side effects are observed in the case of overdose by Ibu systemic administration, including CNS effects ranging from drowsiness to coma.[29] Notably, when Ibu was locally applied in the contused spinal cord with a poly(trimethylene carbonate-co-ε-caprolatone) patch, which produces a 100% drug release over 24 h, RhoA-GTP activity was decreased, demonstrating the local pharmacological activity of the drug.[30]

In order to expand the therapeutic efficacy of Ibu in SCI, we combined it with a promyelinating agent. In fact, white matter injury is generally recognized as a major determinant in outcome after CNS traumatic and vascular lesions, impacting on axons integrity and function, and retrograde neuronal degeneration. Accordingly, remyelination, and specifically the OPCs, became a target for pharmacological as well as cell- and biomaterial-based therapeutic approaches.[31] OPC is, in fact, the cell responsible for myelin repair, and T3 is a key component of the molecular machinery driving cell-cycle exit and terminal differentiation into myelinating oligodendrocyte.[12,32] This process, and subsequently remyelination, is impaired during pathological conditions characterized by severe inflammation, mainly because of the OPC differentiation block, which is sustained by the inflammation-induced rise in cytokine, including tumor necrosis factor alpha, and by alteration of intracellular T3 availability in OPC.[14,33–35]

Different and independent pre-clinical studies in rodents and non-human primates have demonstrated that exogenous TH administration is effective in overcoming the OPCs differentiation block during inflammatory/demyelinating diseases, protecting myelin and axons, and ameliorating the clinical outcome in experimental models of inflammatory/demyelinating diseases.[16,17] However, although T3 crosses the blood–brain barrier by diffusion of by selective transporters, its systemic administration exposes one to the risk of hyperthyroidism and thyroid function suppression.

The designed electrospun scaffold guarantees a local release of the drugs compatible with available data of Ibu and T3 CNS concentration. In fact, CNS tissue concentration of Ibu after systemic administration of 60 mg/kg in constant infusion was $\sim$0.7 μg/g in the rat; the cerebrospinal fluid concentration in humans was $\sim$0.5 μg/mL after a single 800-mg oral administration.[18,36] The physiological T3 concentration in the CNS is $\sim 15\,\mathrm{ng}\times\mathrm{g}^{-1}$ of CNS tissue.[16,17] Moreover, it has been demonstrated that electrospun nanofibrous scaffold of PLLA was not completely degraded up to 12 weeks of implantation s.c. in the rat.[37]

The proposed dual-drug delivery system is intended to be used in acute SCI, to limit secondary neurodegeneration onset and progression by controlling the injured spinal cord microenvironment, thus affecting in cascade glial scar formation, axonal remyelination failure, and, ultimately, functional outcome. To test this hypothesis, we have included several molecular and histological exploratory end points in the study design, starting from glutamate release and macrophage infiltration in spinal cord tissue. It has been reported that after a damaging insult, several mechanisms (e.g., intracellular changes, reversal of glutamate transport, and metabolic alterations) contribute to the massive spontaneous glutamate leakage from nerve terminals.[38–40] On the contrary, K^+-evoked glutamate efflux is mainly associated with the neurosecretory coupling mechanisms leading to the release of the neurotransmitter from the synaptic vesicles. We proved that early (i.e., 24 h after the lesion) spontaneous glutamate release is strongly and specifically reduced in PLLA-Ibu-T3–implanted rats, an effect that appears to be reduced in synaptosomes from tissue dissected 8 days after the lesion. On the contrary, K^+-evoked glutamate efflux is reduced in synaptosomes from tissue dissected from the PLLA-Ibu-T3 group 8 days, but not 24 h, after SCI.

Although other hypotheses cannot be ruled out, it could be speculated that excessive glutamate efflux is mainly attributed to increased glutamate leakage during the primary phase of SCI pathophysiology, while also an increase in neurosecretory coupling mechanisms seems to sustain increased glutamate release during the secondary phase. Interestingly, we proved that both early- and secondary-associated events are reduced in PLLA-Ibu-T3–implanted rats. These effects are considered beneficial in reducing not only neuronal cell death, but particularly in reducing the delayed post-traumatic white matter degeneration in the spinal cord.[41]

We also obtained a partial control of inflammatory infiltrate at the lesion side, and particularly macrophage tissue infiltration and microglia activation, as indicated by the reduction of CD45/CD11b–positive cells. Notably, drug-loaded PLLA also reduces astrogliosis, as measured by flow cytometry of $GLAST^+$ cells at 24 h and 8 days.

This locally delivered drug combination ameliorates the primary end point (BBB score and gait parameters) of efficacy studies. Locomotion parameters in rats implanted with PLLA-Ibu-T3 scaffold are 46% higher than in control rats implanted with drug-unloaded PLLA. This therapeutic efficacy is comparable to even greater than those described in pre-clinical studies supporting ongoing clinical trials.[42,43] In fact, and considering only positive pre-clinical data of drugs in a comparable experimental setting (i.e., in acute SCI) and the same readout (i.e., BBB score at 6–7 weeks), the BBB score amelioration in treated versus control rats was: 33% by methylprednisolone; 23% by ganglioside GM1; 35% by nimodipine; 29% by minocycline; 19% by riluzole; 30% by Rho-kinase inhibitors; 57% by granulocyte colony-stimulating factor; and 17% by anti-Nogo-A antibody. [44–51]

In terms of long-term histopathological outcome, lesion volume was reduced in PLLA-Ibu-T3– compared to PLLA-implanted rats. Several histopathological components are potentially involved in this effect. First of all, the limitation of astroglial reaction also reduces glial fibrillary acidic protein–positive cell density at long term. The multiple roles of astrocytes in brain and spinal cord trauma are known. In the context of SCI, astrocytes are considered a major component of the glial scar, starting activation immediately after SCI and eventually leading to cyst and cavity formation.[52] Myelin, too, is positively affected, in both ascending and descending pathways, indicating that this drug combination and its local concentration protects OPCs, also favoring the full differentiation into myelinating OL. Although there is conflicting evidence in experimental SCI as to whether chronic demyelination is a component of

long-term SCI pathophysiology and functional outcome, extensive literature indicates that oligodendrogenesis and early remyelination exert an important role in protecting axons from long-term degeneration (Preferred Reporting Items for Systematic Reviews and Meta-Analyses [PRISMA] meta-analysis).[53,54]

Overall, this proof-of-concept study leads us to conclude that 1) locally delivered drug combinations should be investigated for their ability to target complex conditions, such as the early phase of the SCI. Notably, when Ibu or T3 are locally delivered as monotherapy in SCI, no long-term functional recovery was observed[55,56]; 2) biomaterial-assisted delivery systems might help to overcome the severe brain diffusion problems, which limits pharmacological interventions; 3) Ibu + T3 delivered locally are able to limit secondary degeneration, leading to a substantial improvement of the functional locomotor outcome; 4) given that these results are obtained by already-marketed drugs and an FDA-approved polymer for tissue implantation, this therapeutic solution could have a shorter regulatory path; and 5) there is also ample room for improvement of this mixed device toward possible clinical application, as different fabrication solution such as micro- and nanoparticles resulting in an injectable solution that could be used in closed spinal cord lesions and in other brain lesions characterized by inflammation and extensive demyelination.

Acknowledgments

Prof. Nadia Passerini (FaBit, University of Bologna) and Prof. Giampiero Pagliuca (DIMEVET, University of Bologna) are gratefully acknowledged for Ibu and T3 assay, respectively. Prof. Maria Laura Bolognesi (FaBit, University of Bologna) is gratefully acknowledged for useful discussion in drug-delivery solution. We thank the patients of the Montecatone Rehabilitation Institute, Montecatone, Imola, Italy, for the continuous stimulus ''from the bedside.'' A special thanks to R.V.

Author Contributions

A.B., A.G., and L.L. performed animal surgery and care, locomotion testing; M.L.F., C.G. performed material design and preparation; M.P. performed Immunohistochemistry and image analysis; A.B. and M.P. performed flow cytometry experiments; S.B. and L.F. performed GABA and glutamate dosage; L.G. contributed to the study design and data analysis; L.C. ideated and designed the study, performed statistical analysis, interpreted the data, and wrote the manuscript.

Funding Information

This work has been supported by the POR-FESR 2014-18, project ''Step-by-Step'', Emilia Romagna Region (to L.C.). The contribution of ''Fondazione Montecatone'', Imola, Italy, and Cluster Tecnologici Nazionali, project IRMI (CTN01_00177_888744), MIUR (to L.C.) are also acknowledged. A special acknowledgment to the GLP-certified CRO TransMed Research srl, who provided the GLP studies for free, in the frame of the ''Step-by-Step'' project.

Author Disclosure Statement

An international patent application from the University of Bologna is pending (PCT/IT2018/000084) (inventors: L.C., L.G., M.L.F., C.G.; no competing financial interests exist for A.B., L.L., A.G., M.P., S.B., L.F.).

References

1. van den Berg, M.E., Castellote, J.M., Mahillo-Fernandez, I., and de Pedro-Cuesta, J. (2010). Incidence of spinal cord injury worldwide: a systematic review. Neuroepidemiology 34, 184–192.
2. Saghazadeh, A., and Rezaei, N, (2017). The role of timing in the treatment of spinal cord injury. Biomed. Pharmacother. 92, 128–139.
3. Rossignol, S., Schwab, M., Schwartz, M., and Fehlings, M.G. (2007). Spinal cord injury: time to move? J. Neurosci. 27, 11782–11792.
4. Hayta, E., Elden, H. (2018). Acute spinal cord injury: a review of pathophysiology and potential of non-steroidal anti-inflammatory drugs for pharmacological intervention. J. Chem. Neuroanat. 87, 25–31.
5. Scholtes, F., Adriaensens, P., Storme, L., Buss, A., Kakulas, A.B., Gelan, J., Beuls, E., Schoenen, J., Brook, G.A., and Martin, D. (2006). Correlation of postmortem 9.4 tesla magnetic resonance imaging and immunohistopathology of the human thoracic spinal cord 7 months after traumatic cervical spine injury. Neurosurgery 59, 671–678.
6. Aarabi, B., Simard, J.M., Kufera, J.A., Alexander, M., Zacherl, K.M., Mirvis, S.E., Shanmuganathan, K., Schwartzbauer, G., Maulucci, C.M., Slavin, J., Ali, K., Massetti, J., and Eisenberg, H.M. (2012). Intramedullary lesion expansion on magnetic resonance imaging in patients with motor complete cervical spinal cord injury. J. Neurosurg. Spine 17, 243–250.
7. Evaniew, N., Belley-Côté, E.P., Fallah, N., Noonan, V.K., Rivers, C.S., and Dvorak, M.F. (2016). Methylprednisolone for the treatment of patients with acute spinal cord injuries: a systematic review and meta-analysis. J. Neurotrauma 33, 468–481.
8. Stahel, P.F., VanderHeiden, T., and Finn, M.A. (2012). Management strategies for acute spinal cord injury: current options and future perspectives. Curr. Opin. Crit. Care 18, 651–660.
9. Shank, C.D., Walters, B.C., and Hadley, M.N., (2017). Management of acute traumatic spinal cord injuries. Handb. Clin. Neurol. 140, 275–298.
10. Wang, X., Budel, S., Baughman, K., Gould, G., Song, K.H., and Strittmatter, S.M. (2009). Ibuprofen enhances recovery from spinal cord injury by limiting tissue loss and stimulating axonal growth. J. Neurotrauma 26, 81–95.
11. Kopp, M.A., Liebscher, T., Watzlawick, R., Martus, P., Laufer, S., Blex, C., Schindler, R., Jungehulsing, G.J., Knüppel, S., Kreutzträger, M., Ekkernkamp, A., Dirnagl, U., Strittmatter S.M., Niedeggen, A., and Schwab, J.M. (2016). SCISSOR-Spinal Cord Injury Study on Small molecule-derived Rho inhibition: a clinical study protocol. BMJ Open 6, e010651.
12. Billon, N., Jolicoeur, C., Tokumoto, Y., Vennström, B, and Raff, M. (2002). Normal timing of oligodendrocyte development depends on thyroid hormone receptor alpha 1 (TRalpha1). EMBO J. 21, 6452–6460.
13. Kuhlmann, T., Miron, V., Cui, Q., Wegner, C., Antel, J., and Brück, W. (2008). Differentiation block of oligodendroglial progenitor cells as a cause for remyelination failure in chronic multiple sclerosis. Brain 131, 1749–1758.
14. Fernández, M., Baldassarro, V.A., Sivilia, S., Giardino, L., and Calzà, L. (2016). Inflammation severely alters thyroid hormone signaling in the central nervous system during experimental allergic encephalomyelitis in rat: direct impact on OPCs differentiation failure. Glia 64, 1573–1589.
15. Calzà, L., Fernández, M., Giuliani, A., Aloe, L., and Giardino, L. (2002). Thyroid hormone activates oligodendrocyte precursors and increases a myelin-forming protein and NGF content in the spinal cord during experimental allergic encephalomyelitis. Proc. Natl. Acad. Sci. U. S. A. 99, 3258–3263.
16. Calzà, L., Fernández, M., and Giardino, L. (2015). Role of the thyroid system in myelination and neural connectivity. Compr. Physiol. 5, 1405–1421.
17. Calzà, L., Baldassarro, V.A., Fernández, M., Giuliani, A., Lorenzini, L., and Giardino, L. (2018). Thyroid hormone and the white matter of the central nervous system: from development to repair. Vitam. Horm. 106, 253–281.
18. Mannila, A., Rautio, J., Lehtonen, M., Järvinen, T., and Savolainen, J. (2005). Inefficient central nervous system delivery limits the use of ibuprofen in neurodegenerative diseases. Eur. J. Pharm. Sci. 24, 101–105.
19. Basso, D.B., Beattie M.S., and Bresnahan, J.C. (1995). A sensitive and reliable locomotor rating scale for open field testing in rats. J. Neurotrauma 12, 1–21.
20. Baldassarro, V.A., Krężel, W., Fernández, M., Schuhbaur, B., Giardino, L., and Calzà, L. (2019). The role of nuclear receptors in the

differentiation of oligodendrocyte precursor cells derived from fetal and adult neural stem cells. Stem Cell Res. 37, 101443.
21. Ozgen, H., Baron, W., Hoekstra. D., and Kahya N. (2016). Oligodendroglial membrane dynamics in relation to myelin biogenesis. Cell. Mol. Life Sci. 73, 3291–3310.
22. Dugas, J.C., Ibrahim, A., and Barres, B.A. (2012). The T3-induced gene KLF9 regulates oligodendrocyte differentiation and myelin regeneration. Mol. Cell. Neurosci. 50, 45–57.
23. Pikov, V., and Wrathall, J.R. (2001). Coordination of the bladder detrusor and the external urethral sphincter in a rat model of spinal cord injury: effect of injury severity. J. Neurosci. 21, 559–569.
24. Watzlawick, R., Sena, E.S., Dirnagl, U., Brommer, B., Kopp, M.A., Macleod, M.R., Howells, D.W., and Schwab, J.M. (2014). Effect and reporting bias of RhoA/ROCK-blockade intervention on locomotor recovery after spinal cord injury: a systematic review and meta-analysis. JAMA Neurol. 71, 91–99.
25. Redondo-Castro, E., and Navarro, X. (2014). Chronic ibuprofen administration reduces neuropathic pain but does not exert neuroprotection after spinal cord injury in adult rats. Exp. Neurol. 252, 95–103.
26. Sharp, K.G., Yee, K.M., Stiles, T.L., Aguilar, R.M., and Steward, O. (2013). A re-assessment of the effects of treatment with a non-steroidal anti-inflammatory (ibuprofen) on promoting axon regeneration via RhoA inhibition after spinal cord injury. Exp. Neurol. 248, 321–337.
27. Streijger, F., Lee, J.H., Duncan, G.J., Ng, M.T., Assinck, P., Bhatnagar, T., Plunet, W.T., Tetzlaff, W., and Kwon, B.K. (2014). Combinatorial treatment of acute spinal cord injury with ghrelin, ibuprofen, C16, and ketogenic diet does not result in improved histologic or functional outcome. J. Neurosci. Res. 92, 870–883.
28. Parepally, J.M., Mandula, H., and Smith, Q.R. (2006). Brain uptake of nonsteroidal anti-inflammatory drugs: ibuprofen, flurbiprofen, and indomethacin. Pharm. Res. 23, 873–881.
29. Auriel, E., Regev, K., and Korczyn, A.D. (2014). Nonsteroidal anti-inflammatory drugs exposure and the central nervous system. Handb. Clin. Neurol. 119, 577–584.
30. Pires, L.R., Lopes, C.D.F., Salvador, D., Rocha, D.N., and Pêgo, A.P. (2017). Ibuprofen-loaded fibrous patches-taming inhibition at the spinal cord injury site. J. Mater. Sci. Mater. Med. 28, 157.
31. Chew, L.J., and DeBoy, C.A. (2016). Pharmacological approaches to intervention in hypomyelinating and demyelinating white matter pathology. Neuropharmacology 110, 605–625.
32. Lee, J.Y., and Petratos, S. (2016). Thyroid hormone signaling in oligodendrocytes: from extracellular transport to intracellular signal. Mol. Neurobiol. 53, 6568–6583.
33. Hassannejad, Z., Shakouri-Motlagh, A., Mokhatab, M., Zadegan, S.A., Sharif-Alhoseini, M., Shokraneh, F., and Rahimi-Movaghar, V. (2019). Oligodendrogliogenesis and axon remyelination after traumatic spinal cord injuries in animal studies: a systematic review. Neuroscience 402, 37–50.
34. Billiards, S.S., Haynes, R.L., Folkerth, R.D., Borenstein, N.S., Trachtenberg, F.L., Rowitch, D.H., Ligon, K.L., Volpe, J.J., and Kinney, H.C. (2008). Myelin abnormalities without oligodendrocyte loss in periventricular leukomalacia. Brain Pathol. 18, 153–163.
35. Valentin-Torres, A., Savarin, C., Barnett, J., and Bergmann, C.C. (2018). Blockade of sustained tumor necrosis factor in a transgenic model of progressive autoimmune encephalomyelitis limits oligodendrocyte apoptosis and promotes oligodendrocyte maturation. J. Neuroinflammation 15, 121.
36. Bannwarth, B., Lapicque, F., Pehourcq, F., Gillet, P., Schaeverbeke, T., Laborde, C., Dehais, J., Gaucher, A., and Netter, P. (1995). Stereoselective disposition of ibuprofen enantiomers in human cerebrospinal fluid. Br. J. Clin. Pharmacol. 40, 266–269.
37. Ishii, D., Ying, T.H., Mahara, A., Murakami, S., Yamaoka, T., Lee, W.K., and Iwata, T. (2009). In vivo tissue response and degradation behavior of PLLA and stereocomplexed PLA nanofibers. Biomacromolecules 10, 237–242.
38. Phillis, J.W., and O'Regan, MH. (1996). Mechanisms of glutamate and aspartate release in the ischemic rat cerebral cortex. Brain Res. 730, 150–164.
39. Li, S., Mealing, G.A., Morley, P., and Stys, P.K. (1999). Novel injury mechanism in anoxia and trauma of spinal cord white matter: glutamate release via reverse Na+-dependent glutamate transport. J. Neurosci. 19, RC16.
40. Sheldon, A.L., and Robinson, M.B. (2007). The role of glutamate transporters in neurodegenerative diseases and potential opportunities for intervention. Neurochem. Int. 51, 333–355.
41. Park, E., Velumian, A.A., and Fehlings, M.G. (2004). The role of excitotoxicity in secondary mechanisms of spinal cord injury: a review with an emphasis on the implications for white matter degeneration. J. Neurotrauma 21, 754–774.
42. Badhiwala, J.H., Ahuja, C.S., and Fehlings M.G. (2018). Time is spine: a review of translational advances in spinal cord injury. J. Neurosurg. Spine 30, 1–18.
43. Gomes-Osman, J., Cortes, M., Guest, J., and Pascual-Leone, A. (2019). Systematic review of experimental strategies aimed at improving motor function after acute and chronic spinal cord injury. J. Neurotrauma 33, 425–438.
44. Liu, D., Shan, Y., Valluru, L., and Bao, F. (2013). Mn (III) tetrakis (4-benzoic acid) porphyrin scavenges reactive species, reduces oxidative stress, and improves functional recovery after experimental spinal cord injury in rats: comparison with methylprednisolone. BMC Neurosci. 14, 23.
45. Marcon, R.M., Cristante, A.F., de Barros Filho, T.E., de Oliveira, R.P., and dos Santos, G.B. (2010). Potentializing the effects of GM1 by hyperbaric oxygen therapy in acute experimental spinal cord lesion in rats. Spinal Cord 48, 808–813.
46. Jia, Y.F., Gao, H.L., Ma, L.J., and Li, J. (2015). Effect of nimodipine on rat spinal cord injury. Genet. Mol. Res. 14, 1269–1276.
47. Ahmad, M., Zakaria, A., and Almutairi, K.M. (2016). Effectiveness of minocycline and FK506 alone and in combination on enhanced behavioral and biochemical recovery from spinal cord injury in rats. Pharmacol. Biochem. Behav. 145, 45–54.
48. Mu, X., Azbill, R.D., and Springer, J.E. (2000). Riluzole and methylprednisolone combined treatment improves functional recovery in traumatic spinal cord injury. J. Neurotrauma 17, 773–780.
49. Dergham, P., Ellezam, B., Essagian, C., Avedissian, H., Lubell, W.D., and McKerracher, L. (2002). Rho signalling pathway targeted to promote spinal cord repair. J. Neurosci. 22, 6570–6577.
50. Chen, W.F., Chen, C.H., Chen, N.F., Sung, C.S., and Wen, Z.H. (2015). Neuroprotective effects of direct intrathecal administration of granulocyte colony-stimulating factor in rats with spinal cord injury. CNS Neurosci. Ther. 21, 698–707.
51. Liebscher, T., Schnell, L., Schnell, D., Scholl, J., Schneider, R., Gullo, M., Fouad, K,. Mir, A., Rausch, M., Kindler, D., Hamers, F.P., and Schwab, M.E. (2005). Nogo-A antibody improves regeneration and locomotion of spinal cord-injured rats. Ann. Neurol. 58, 706–719.
52. Okada, S., Hara, M., Kobayakawa, K., Matsumoto, Y., and Nakashima, Y. (2018). Astrocyte reactivity and astrogliosis after spinal cord injury. Neurosci. Res. 126, 39–43.
53. Duncan, G.J., Manesh, S.B., Hilton, B.J., Assinck, P., Liu, J., Moulson, A., Plemel, J.R., and Tetzlaff, W. (2018). Locomotor recovery following contusive spinal cord injury does not require oligodendrocyte remyelination. Nat. Commun. 9, 3066.
54. Hassannejad, Z., Shakouri-Motlagh, A., Mokhatab, M., Zadegan, S.A., Sharif-Alhoseini, M., Shokraneh, F., and Rahimi-Movaghar, V. (2019). Oligodendrogliogenesis and axon remyelination after traumatic spinal cord injuries in animal studies: a systematic review. Neuroscience 402, 37–50.
55. Qi, L., Jiang, H., Cui, X., Liang, G., Gao, M., Huang, Z., and Xi, Q. (2017). Synthesis of methylprednisolone loaded ibuprofen modified dextran based nanoparticles and their application for drug delivery in acute spinal cord injury. Oncotarget 8, 99666–99680.
56. Shultz, R.B., Wang, Z., Nong, J., Zhang, Z., and Zhong, Y. (2017). Local delivery of thyroid hormone enhances oligodendrogenesis and myelination after spinal cord injury. J. Neural Eng. 14, 036014.

Address correspondence to:
Laura Calzà, MD
CIRI-SDV and FaBit
University of Bologna
Via Tolara di Sopra 41/E
40064 Ozzano Emilia, Bologna
Italy

E-mail: laura.calza@unibo.it